

Decoherence under many-body system-environment interactions: a stroboscopic representation based on a fictitiously homogenized interaction rate

Gonzalo A. Álvarez, Ernesto P. Danieli, Patricia R. Levstein, and Horacio M. Pastawski*
Facultad de Matemática, Astronomía y Física, Universidad Nacional de Córdoba, 5000 Córdoba, Argentina

An environment interacting with portions of a system leads to multiexponential interaction rates. Within the Keldysh formalism, we fictitiously homogenize the system-environment interaction yielding a uniform decay rate facilitating the evaluation of the propagators. Through an injection procedure we neutralize the fictitious interactions. This technique justifies a stroboscopic representation of the system-environment interaction which is useful for numerical implementation and converges to the natural continuous process. We apply this procedure to a fermionic two-level system and use the Jordan-Wigner transformation to solve a two-spin swapping gate in the presence of a spin environment.

PACS numbers: 03.65.Yz, 03.65.Ta, 03.65.Xp, 76.60.-k

I. INTRODUCTION

The control of open quantum systems has a fundamental relevance for fields ranging from quantum information processing (QIP) [1] to nanotechnology [2, 3, 4]. Typically, the system whose coherent dynamics one wants to manipulate, interacts with an environment that smoothly degrades its quantum dynamics. This process, called “decoherence”, can even be assisted by the own system’s complexity [5]. Since environment induced decoherence [6, 7, 8] constitutes the main obstacle towards QIP, a precise understanding of its inner mechanisms [2, 9, 10] is critical to develop strategies to control the quantum dynamics.

The usual way to obtain the dynamics is to solve a generalized Liouville-von Neumann differential equation for the reduced density matrix. There the degrees of freedom of the environment are traced out to yield a quantum master equation (QME) [11]. A less known alternative is provided by the Keldysh formalism [12] in the integral representation proposed by Danielewicz [13]. On one side, it uses the well known perturbation to infinite order in selected terms provided by the Feynman diagrams. On the other, this integral representation has the advantage of being able to profit from a Wigner representation is particularly meaningful in the fermionic case since it allows ones to define energy states and their occupations simultaneously with the physical time [14]. In that case, one can transform the Danielewicz equation into the generalized Landauer-Büttiker equation (GLBE) [14, 15] to solve the quantum dynamics of the system. When the system-environment (SE) interaction is spatially homogeneous, i.e., it has an equal interaction with each component of the system, the dynamics becomes particularly simple because there is a uniform SE interaction rate. However, there are many situations where one should incorporate

multiple rates as different subsets of the system could suffer diverse interaction processes. While this might not possess a great challenge to the evaluation of steady state transport properties, in quantum dynamics, one is confronted with what appears to be a much more difficult problem. Here, we present a procedure to convert a nonhomogeneous problem with multiple SE interaction rates, into one that has a common rate. Through a reinjection procedure, we instantaneously neutralize the fictitious decays restoring the populations and, eventually, the coherences. In order to illustrate the procedure, we apply this technique to a model that represents a single fermion that can jump between two states while an external fermionic reservoir is coupled to one of them. This provides decoherence due to a through space Coulomb interaction and can feed with an extra particle through tunneling processes. While the parameters and approximations involved in this model are especially designed to be mapped to a problem of spin dynamics, it could also be adapted to represent a double quantum dot charge qubit [16]. In that case a double dot is operated in the gate voltage regime where there is a single electron which can jump between the two coupled states, where only one of these states is coupled to an electron reservoir. This inhomogeneous SE interaction yields a multiexponential decay rate. We introduce fictitious interactions to obtain a common interaction rate which leads to a homogeneous non-Hermitian effective Hamiltonian. In the specific model considered, we analyze how different SE interactions, e.g., tunneling to the leads and through space Coulomb interaction, modify the quantum evolution. A particular advantage of the fictitious symmetrization is that it leads naturally to a stroboscopic representation of the SE processes. This leads to a very efficient numerical algorithm where the quantum dynamics is obtained in a sequence of time steps. Finally, we resort to the Jordan-Wigner mapping between fermions and spins to apply the procedure to a spin system. This allows us to give a first-principle derivation of the self-energies used in the stroboscopic model introduced in Ref. [17] to explain the puzzling experimental dynamics observed [18] in a spin swapping gate [19].

*Electronic address: horacio@famaf.unc.edu.ar

II. SYSTEM

Let us consider an electron in a two-state system asymmetrically coupled to an electron reservoir, as shown in Fig. 1(a), with the total Hamiltonian $\hat{\mathcal{H}} = \hat{\mathcal{H}}_S + \hat{\mathcal{H}}_E + \hat{\mathcal{H}}_{SE}$.

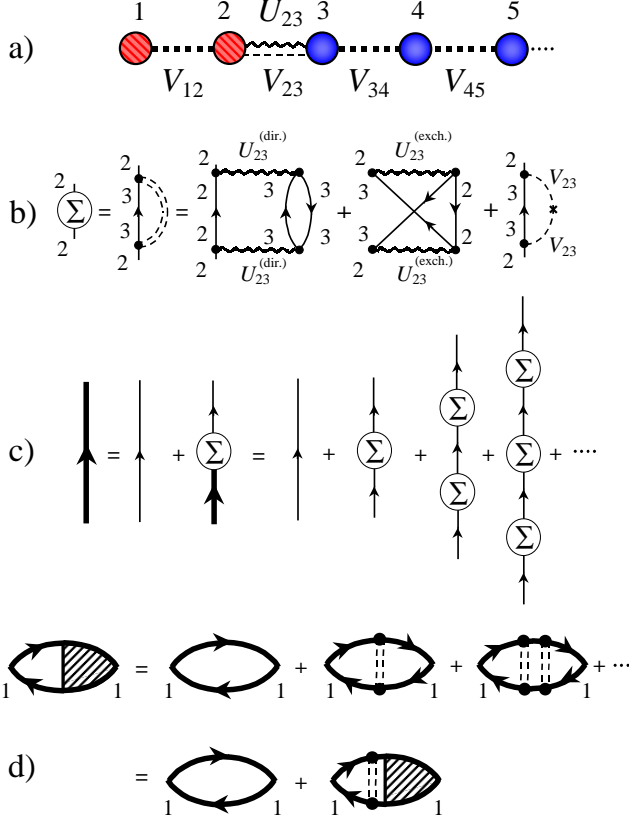


FIG. 1: (Color online) (a) System-environment (SE) representation. Dashed circles and solid circles represent the system and the environment states respectively. Dashed lines are hopping interactions while wiggly lines are through-space Coulomb interactions. (b) Self-energy diagram summing up the different interactions with the environment in a local basis. The lines with arrows are exact Green's functions in the absence of SE interactions. The double dashed line represents the effective SE interaction. (c) Retarded Green's function at site 1. The interaction with the environment is to infinite order in the self-energy given in (b). (d) Particle density function at site 1. The double dashed lines represent the effective interactions local in time and space summed up to infinity order.

The system Hamiltonian is

$$\hat{\mathcal{H}}_S = E_1 \hat{c}_1^\dagger \hat{c}_1 + E_2 \hat{c}_2^\dagger \hat{c}_2 - V_{12} (\hat{c}_1^\dagger \hat{c}_2 + \hat{c}_2^\dagger \hat{c}_1), \quad (1)$$

with \hat{c}_i^\dagger (\hat{c}_i) the standard fermionic creation (destruction) operators. The E_i are the energies of the i -th local state

whose spin index is omitted. The hopping interaction V_{12} gives the natural frequency $\omega_0 = 2V_{12}/\hbar$ of the transition between the states 1 and 2. The environment has a similar Hamiltonian,

$$\hat{\mathcal{H}}_E = \sum_{i=3}^{\infty} E_i \hat{c}_i^\dagger \hat{c}_i - \sum_{\substack{i,j=3 \\ i \neq j}}^{\infty} V_{ij} (\hat{c}_i^\dagger \hat{c}_j + \hat{c}_j^\dagger \hat{c}_i), \quad (2)$$

where the V_{ij} determines the topology of the interaction network in the environment states. The system-environment interaction is described by

$$\begin{aligned} \hat{\mathcal{H}}_{SE} = \sum_{\alpha=\uparrow,\downarrow} \left\{ \sum_{\beta=\uparrow,\downarrow} U_{23}^{(\text{dir.})} \hat{c}_{2\beta}^\dagger \hat{c}_{2\beta} \hat{c}_{3\alpha}^\dagger \hat{c}_{3\alpha} \right. \\ \left. + U_{23}^{(\text{exch.})} \hat{c}_{2\alpha}^\dagger \hat{c}_{3\alpha} \hat{c}_{3\alpha}^\dagger \hat{c}_{2\alpha} - V_{23} (\hat{c}_{2\alpha}^\dagger \hat{c}_{3\alpha} + \hat{c}_{3\alpha}^\dagger \hat{c}_{2\alpha}) \right\}, \quad (3) \end{aligned}$$

The first two terms on the rhs represent the Coulomb interaction of an electron in site 2 with an electron in site 3, the first site of the reservoir. $U_{23}^{(\text{dir.})}$ is the standard direct integral and $U_{23}^{(\text{exch.})}$ is the small exchange integral which we include for completeness. The third term is the hopping interaction between sites 2 and 3.

III. SYSTEM EVOLUTION

A. Quantum dynamics in the Keldysh formalism

We are interested in the study of the evolution of an initial local excitation in the system. Let us consider the initial excitation with a particle on site 2 and a hole in site 1 which is described by the non-equilibrium state,

$$|\Psi_{\text{n.e.}}\rangle = \hat{c}_2^\dagger \hat{c}_1 |\Psi_{\text{eq.}}\rangle, \quad (4)$$

where $|\Psi_{\text{eq.}}\rangle$ is the thermodynamical many-body equilibrium state at high temperatures which is the regime of NMR spin dynamics. In this condition $|\Psi_{\text{eq.}}\rangle$ is the mixture, with equal weight, of all the possible Slater determinants [20]. The evolution in a complete norm preserving solution is described by the particle and hole density functions

$$G_{ij}^<(t_2, t_1) = \frac{i}{\hbar} \langle \Psi_{\text{n.e.}} | \hat{c}_j^\dagger(t_1) \hat{c}_i(t_2) | \Psi_{\text{n.e.}} \rangle \quad (5)$$

and

$$G_{ij}^>(t_2, t_1) = -\frac{i}{\hbar} \langle \Psi_{\text{n.e.}} | \hat{c}_i(t_2) \hat{c}_j^\dagger(t_1) | \Psi_{\text{n.e.}} \rangle, \quad (6)$$

that describe spatial and temporal correlations. In these expressions, the creation and destruction operators are in the Heisenberg representation. Notice that in contrast with the equilibrium definitions of $G_{ij}^< (t_2, t_1)$, now they have an implicit dependence on the initial local excitation. The probability amplitude of finding a particle in

site i at time t_2 when it initially was in site j at time t_1 is described by the retarded Green's function of the whole system

$$\begin{aligned} G_{ij}^R(t_2, t_1) &= \theta(t_2, t_1) [G_{ij}^>(t_2, t_1) - G_{ij}^<(t_2, t_1)] \\ &= [G_{ji}^A(t_1, t_2)]^*. \end{aligned} \quad (7)$$

The reduced density function $\mathbf{G}^<(t, t)$, where matrix indices are restricted to $i, j \in \{1, 2\}$, is equivalent to the single particle 2×2 density matrix and $\mathbf{G}^R(t_2, t_1)$ is an effective evolution operator [21]. If the system is isolated, the Green's function in its energy representation is obtained by a Fourier transform (FT) with respect to the time interval $\delta t = t_2 - t_1$,

$$\mathbf{G}^{\text{OR}}(\varepsilon, t) = \int \mathbf{G}^{\text{OR}}(t + \frac{1}{2}\delta t, t - \frac{1}{2}\delta t) \exp[i\varepsilon\delta t/\hbar] d\delta t, \quad (8)$$

where $t = \frac{1}{2}(t_2 + t_1)$. In a time independent system

$$\mathbf{G}^{\text{OR}}(\varepsilon, t) \equiv \mathbf{G}^{\text{OR}}(\varepsilon) = [\varepsilon \mathbf{I} - \mathbf{H}_S]^{-1}. \quad (9)$$

After including SE interactions, the Green's function defines the reduced effective Hamiltonian and the self-energy $\Sigma^R(\varepsilon)$ [22],

$$\mathbf{H}_{\text{eff}}(\varepsilon) \equiv \varepsilon \mathbf{I} - [\mathbf{G}^R(\varepsilon)]^{-1} = \mathbf{H}_S + \Sigma^R(\varepsilon). \quad (10)$$

Here, the exact perturbed dynamics is contained in the nonlinear dependence of the self-energy Σ^R on ε . For infinite reservoirs the evolution with \mathbf{H}_{eff} is nonunitary, hence, the Green's function has poles at the “eigenenergies”, ε_ν , that have imaginary components [23],

$$-2 \text{Im} \Sigma^R(\varepsilon_\nu) / \hbar = 1/\tau_{\text{SE}} = 2\Gamma_{\text{SE}}/\hbar. \quad (11)$$

These account for the “decay rates” into collective SE eigenstates in agreement with a self-consistent Fermi golden rule (FGR) [24]. Similarly, $\text{Re} \Sigma^R(\varepsilon_\nu) = \text{Re} \varepsilon_\nu - \varepsilon_\nu^0$ represent the “shifts” of the system's eigenenergies ε_ν^0 .

The evolution of the density function for the reduced open system is described using the Keldysh formalism [12, 13]. The density function in the Danielewicz form [13] is

$$\begin{aligned} \mathbf{G}^<(t_2, t_1) &= \hbar^2 \mathbf{G}^R(t_2, 0) \mathbf{G}^<(0, 0) \mathbf{G}^A(0, t_1) \\ &+ \int_0^{t_2} \int_0^{t_1} dt_k dt_l \mathbf{G}^R(t_2, t_k) \Sigma^<(t_k, t_l) \mathbf{G}^A(t_l, t_1). \end{aligned} \quad (12)$$

The first term is the “coherent” evolution while the second term contains “incoherent reinjections” through the self-energy function $\Sigma^<$. This compensates any leak from the coherent evolution reflected by the imaginary part of Σ^R (see [14]). We remark that this expression is valid for a noncorrelated initial state which is our case of interest. For a correlated state see Ref. [25]. The key to solve Eq. (12) is to build up an expression for the particle (hole) injection and retarded self-energies $\Sigma^{<(>)}(t_1, t_2)$ and

$$\Sigma^R(t_1, t_2) = \theta(t_1, t_2) [\Sigma^>(t_2, t_1) - \Sigma^<(t_2, t_1)]. \quad (13)$$

For this purpose, we use a perturbative expansion on \mathcal{H}_{SE} like that used in Ref. [26] for the Coulomb interaction and in Ref. [27] for the hopping interaction. The first order in the perturbation expansion is the standard Hartree-Fock energy correction which does not contribute to $\Sigma^<$ because it is real. We focus on the second-order terms, with Feynman diagrams sketched in Fig. 1(b).

The injection self-energy is

$$\begin{aligned} \Sigma_{ij}^<(t_k, t_l) &= \\ |U_{23}|^2 \hbar^2 G_{33}^<(t_k, t_l) G_{33}^>(t_l, t_k) G_{22}^<(t_k, t_l) \delta_{i2} \delta_{2j} \\ &+ |V_{23}|^2 G_{33}^<(t_k, t_l) \delta_{i2} \delta_{2j}, \end{aligned} \quad (14)$$

where $U_{23} = -2U_{23}^{(\text{dir.})} + U_{23}^{(\text{exch.})}$ is the net Coulomb interaction between an electron in the system and one in the reservoir. The direct term contributes with a fermion loop and an extra spin summation which is represented in the -2 factor [13]. The first term in Eq. (14) corresponds to the direct and exchange self-energy diagrams shown in the last line of Fig. 1(b). The first two diagrams schematize the creation of an electron-hole pair in the environment and its later destruction. The last term in Eq. (14) and the last diagram of the same figure is the hopping to site 3 which allows the electron to perform a full exploration inside the reservoir. To take into account the different time scales for the dynamics of excitations in the system and in the reservoir, we use the energy-time variables: the physical time $t_i = \frac{1}{2}(t_k + t_l)$, and the domain of quantum correlations $\delta t_i = t_k - t_l$. This last is related to an energy ε through a FT [14]. Thus, in equilibrium,

$$G_{33}^<(\varepsilon, t_i) = i2\pi N_3(\varepsilon) f_3(\varepsilon, t_i), \quad (15)$$

$$G_{33}^>(\varepsilon, t_i) = -i2\pi N_3(\varepsilon) [1 - f_3(\varepsilon, t_i)], \quad (16)$$

where $N_3(\varepsilon)$ is the local density of states (LDoS) at the surface of the reservoir. Assuming that the environment stays in the thermodynamical equilibrium and $k_B T$ is much higher than any energy scale in the bath (high temperature limit), the occupation factor is

$$f_3(\varepsilon, t_i) = f_3. \quad (17)$$

Fourier transforming on ε one obtains

$$G_{33}^<(t_i + \frac{\delta t_i}{2}, t_i - \frac{\delta t_i}{2}) = i2\pi g_3(\delta t_i) f_3 \quad (18)$$

and

$$G_{33}^>(t_i + \frac{\delta t_i}{2}, t_i - \frac{\delta t_i}{2}) = -i2\pi g_3(\delta t_i) (1 - f_3), \quad (19)$$

where

$$g_3(\delta t_i) = \int N_3(\varepsilon) e^{-i\varepsilon\delta t_i} \frac{d\varepsilon}{2\pi\hbar}. \quad (20)$$

Replacing in Eq. (14)

$$\begin{aligned} \Sigma_{ij}^{\leq}(t_i + \frac{\delta t_i}{2}, t_i - \frac{\delta t_i}{2}) = & \\ & |U_{23}|^2 \hbar^2 (2\pi)^2 [g_3(\delta t_i)]^2 f_3 [1 - f_3] \\ & \times G_{22}^{\leq}(t_i + \frac{\delta t_i}{2}, t_i - \frac{\delta t_i}{2}) \delta_{i2} \delta_{2j} \\ & \pm |V_{23}|^2 i 2\pi g_3(\delta t_i) \begin{pmatrix} f_3 \\ 1 - f_3 \end{pmatrix} \delta_{i2} \delta_{2j}, \end{aligned} \quad (21)$$

where the $\begin{pmatrix} f_3 \\ 1 - f_3 \end{pmatrix}$ associates f_3 with $\Sigma^<$ and $(1 - f_3)$ with $\Sigma^>$.

In summary, we are left with the task to evaluate the time dependent self-energies and the integral in Eq. (12). We will focus on the parametric regime corresponding to the experimental conditions of the spin swapping gate.

B. Environment in the wide band or fast fluctuations regime

As occurs with the generalized Landauer-Büttiker equations for linear transport, an essential ingredient is the possibility to assign a Markovian nature to the environment. We are going to see that this appears naturally from the formalism when the dynamics of excitations within the environment is faster than the time scales relevant to the system. In order to separate the different physical time scales involved in the problem, we start changing to the energy-time variables in Eq. (12). Evaluating in $t_2 = t_1 = t$, the integrand becomes

$$\begin{aligned} & \int_0^t dt_i \int_{-t}^t d\delta t_i \\ & \times G^R(t, t_i + \frac{\delta t_i}{2}) \Sigma^<(t_i + \frac{\delta t_i}{2}, t_i - \frac{\delta t_i}{2}) G^A(t_i - \frac{\delta t_i}{2}, t). \end{aligned} \quad (22)$$

The environment unperturbed Green's function $g_3(\delta t_i)$ decays within the time scale \hbar/V_B where V_B is the characteristic interaction inside the reservoir. In the wide band regime ($V_B \gg V_{12}$) \hbar/V_B becomes much shorter than the characteristic evolution time of $G_{22}^{\leq}(t_i + \frac{\delta t_i}{2}, t_i - \frac{\delta t_i}{2})$ given by \hbar/V_{12} . Then, as the main contribution to the integral on δt_i of Eq. (12) is around the time scale \hbar/V_B we can replace $G_{22}^{\leq}(t_i + \frac{\delta t_i}{2}, t_i - \frac{\delta t_i}{2})$ by $G_{22}^{\leq}(t_i, t_i)$. Following the same assumption we replace $G^R(t, t_i + \frac{\delta t_i}{2})$ by $G^R(t, t_i)$ and $G^A(t_i - \frac{\delta t_i}{2}, t)$ by $G^A(t_i, t)$. In this fast fluctuation regime, only $\Sigma_{ij}^{\leq}(t_i + \frac{\delta t_i}{2}, t_i - \frac{\delta t_i}{2})$ depends on

δt_i leading to

$$\begin{aligned} \Sigma_{ij}^{\leq}(t_i) = & \int_{-t}^t \Sigma_{ij}^{\leq}(t_i + \frac{\delta t_i}{2}, t_i - \frac{\delta t_i}{2}) d\delta t_i \\ = & |U_{23}|^2 \hbar^2 (2\pi)^2 \left[\int_{-t}^t [g_3(\delta t_i)]^2 d\delta t_i \right] f_3 [1 - f_3] \\ & \times G_{22}^{\leq}(t_i, t_i) \delta_{i2} \delta_{2j} \\ \pm & |V_{23}|^2 i 2\pi \left[\int_{-t}^t g_3(\delta t_i) d\delta t_i \right] \begin{pmatrix} f_3 \\ 1 - f_3 \end{pmatrix} \delta_{i2} \delta_{2j}, \end{aligned} \quad (23)$$

which is local in space and time. Here, because of the limit $V_{12}/V_B \rightarrow 0$, the correlation function of site 3 becomes a representation of the Dirac delta function. Thus, any perturbation at site 3 is almost instantaneously spread all over the environment (as compared with the time scale of the system dynamics) and hence the occupation at site 3 remains constant. This assumption for the time scales can be seen in Fig. 1(b) as a collapse of a pair of black dots, along a vertical line, into a single point. This justifies the expansion of Fig. 1(c) and the use of the ladder approximation containing only vertical interaction lines in Fig. 1(d).

A generalized decay rate is given by

$$1/\tau_{SE}(\varepsilon, t_i) \equiv 2\Gamma_{SE}(\varepsilon, t_i)/\hbar \equiv -2\text{Im} \Sigma^R(\varepsilon, t_i)/\hbar \quad (24)$$

$$= \frac{i}{\hbar} [\Sigma_{22}^A(\varepsilon, t_i) - \Sigma_{22}^R(\varepsilon, t_i)] \quad (25)$$

$$= \frac{i}{\hbar} [\Sigma_{22}^>(\varepsilon, t_i) - \Sigma_{22}^<(\varepsilon, t_i)], \quad (26)$$

where

$$\Sigma_{ij}^{\leq}(\varepsilon, t_i) = \int_{-\infty}^{\infty} \Sigma_{ij}^{\leq}(t_i + \frac{\delta t_i}{2}, t_i - \frac{\delta t_i}{2}) e^{i\varepsilon \delta t_i/\hbar} d\delta t_i. \quad (27)$$

We start assuming $E_i = 0$ for $i = 1, \dots, \infty$, so the only relevant energy scale of the system is $V_{12} \ll V_B$. As mentioned above, in the wide band limit the correlation function $g_3(\delta t_i)$ becomes a representation of the Dirac delta function. In this way, the term $e^{i\varepsilon \delta t_i/\hbar}$ of the integrand of Eq. (27) is evaluated for $\delta t_i = 0$ giving a value equal to 1. Thus, using Eq. (23), we obtain for the decay rate which in the wide band limit is constant in time and independent of energy,

$$\frac{1}{\tau_{SE}} \underset{\text{WB}}{=} \frac{i}{\hbar} [\Sigma_{22}^>(t_i) - \Sigma_{22}^<(t_i)] \quad (28)$$

$$\begin{aligned} = & |U_{23}|^2 (2\pi)^2 \left[\int_{-t}^t [g_3(\delta t_i)]^2 d\delta t_i \right] f_3 [1 - f_3] \\ & + \frac{1}{\hbar} |V_{23}|^2 2\pi \left[\int_{-t}^t g_3(\delta t_i) d\delta t_i \right] \end{aligned} \quad (29)$$

$$= \frac{2}{\hbar} (\Gamma_U + \Gamma_V), \quad (30)$$

where we have used $t \gg \hbar/V_B$ to equal $\Sigma_{ij}^{\leq}(\varepsilon, t_i) = \Sigma_{ij}^{\leq}(t_i)$ and define

$$\Gamma_U = \hbar |U_{23}|^2 2\pi^2 \left[\int_{-\infty}^{\infty} [g_3(\delta t_i)]^2 d\delta t_i \right] f_3 [1 - f_3], \quad (31)$$

the Coulomb decay rate, and

$$\Gamma_V = |V_{23}|^2 \pi \left[\int_{-\infty}^{\infty} g_3(\delta t_i) d\delta t_i \right], \quad (32)$$

the hopping decay rate. If one assumes that the environment (2) can be represented by a linear chain with near neighbor hoppings equal to V_B and $E_i \equiv 0$, the LDoS is (see Ref. [27])

$$N_3(\varepsilon) = 1/(\pi V_B) \sqrt{1 - \left(\frac{\varepsilon}{2V_B}\right)^2}. \quad (33)$$

Thus, the Green's function

$$g_3(\delta t_i) = \frac{1}{2\pi V_B} \frac{J_1\left(\frac{2V_B}{\hbar}\delta t_i\right)}{\delta t_i} \quad (34)$$

is proportional to the first-order Bessel function and decays within a characteristic time \hbar/V_B . Assuming that $f_3 = 1/2$ and the integration limits in the Γ 's expressions are taken to infinity because $t \sim \hbar/V_{12} \gg \hbar/V_B$ (wide band approximation), one obtains

$$\frac{2}{\hbar}\Gamma_U = \frac{2\pi}{\hbar} |U_{23}|^2 \frac{2}{3\pi^2 V_B} \quad (35)$$

and

$$\frac{2}{\hbar}\Gamma_V = \frac{2\pi}{\hbar} |V_{23}|^2 \frac{1}{\pi V_B}. \quad (36)$$

Since the interaction is local in time, the reduced density results as follows

$$\mathbf{G}^<(t, t) = \hbar^2 \mathbf{G}^R(t, 0) \mathbf{G}^<(0, 0) \mathbf{G}^A(0, t) + \int_0^t dt_i \mathbf{G}^R(t, t_i) \mathbf{\Sigma}^<(t_i) \mathbf{G}^A(t_i, t), \quad (37)$$

which is complemented with

$$\mathbf{\Sigma}^<(t_i) = \begin{pmatrix} 0 & 0 \\ 0 & 2\Gamma_U \hbar G_{22}^<(t_i, t_i) + 2\Gamma_V \hbar \left(\frac{i}{\hbar} f_3\right) \end{pmatrix}. \quad (38)$$

Here, the propagators $\mathbf{G}^R(t, 0)$ and $\mathbf{G}^A(0, t)$ that enter in both terms are obtained from the effective Hamiltonian of the reduced system,

$$\mathbf{H}_{\text{eff.}} = \begin{pmatrix} 0 & -V_{12} \\ -V_{12} & -i\Gamma_{\text{SE}} \end{pmatrix}, \quad (39)$$

where Γ_{SE} is energy independent and the assumption $E_i = 0$ for all i assures that the self-energies are purely imaginary. This effective Hamiltonian is obtained from Eq. (10) and using Eq. (13) previously converted into the energy-time variables. This means that we first change the variables (t_1, t_2) to $(t_i, \delta t_i)$ and then based on a Fourier transform on δt_i we obtain the energy-time representation which results in the independence on both ε and t_i .

The above procedure results in an equation of the form of the GLBE. However, the Hamiltonian is asymmetric in the SE interaction complicating the form of the associated propagator. The apparent complexity to solve this equation contrasts with the homogeneous case where the evolution of the GLBE was obtained [15] through a Laplace transform. Our strategy will be to induce such a form of symmetry.

C. Fictitious homogeneous decay

The main difficulty with Eq. (37) is that it involves multiple exponentials. In order to create propagators with an homogeneous decay, i.e., a single exponential factor, we introduce *fictitious interactions* $\mathbf{\Sigma}_{\text{fic.}}^R$ with the environment. The symmetric Hamiltonian becomes

$$\begin{aligned} \mathbf{H}_{\text{sym.}} &= \mathbf{H}_{\text{eff.}} + \mathbf{\Sigma}_{\text{fic.}}^R \\ &= \begin{pmatrix} 0 & -V_{12} \\ -V_{12} & -i\Gamma_{\text{SE}} \end{pmatrix} + \begin{pmatrix} -i\frac{1}{2}\Gamma_{\text{SE}} & 0 \\ 0 & i\frac{1}{2}\Gamma_{\text{SE}} \end{pmatrix} \\ &= \begin{pmatrix} -i\frac{1}{2}\Gamma_{\text{SE}} & -V_{12} \\ -V_{12} & -i\frac{1}{2}\Gamma_{\text{SE}} \end{pmatrix}. \end{aligned} \quad (40)$$

Here $\mathbf{\Sigma}_{\text{fic.}}^R$ includes the fictitious interactions which, in the present case, produce a *leak of probability* in site 1 at a rate Γ_{SE}/\hbar while in site 2 *inject probability* at the same rate. Both states of $\mathbf{H}_{\text{sym.}}$ interact with the environment independently with the same characteristic decay rate Γ_{SE}/\hbar . Note that this rate is half the real value. The propagators of Eq. (12) have now a simple dependence on t as

$$\mathbf{G}^R(t, 0) = \mathbf{G}^{\text{OR}}(t, 0) e^{-\frac{\Gamma_{\text{SE}}}{2} t/\hbar}, \quad (41)$$

where

$$G_{11}^{\text{OR}}(t, 0) = G_{22}^{\text{OR}}(t, 0) = \frac{i}{\hbar} \cos\left(\frac{\omega_0}{2} t\right) \quad (42)$$

and

$$G_{12}^{\text{OR}}(t, 0) = G_{21}^{\text{OR}}(t, 0)^* = \frac{i}{\hbar} \sin\left(\frac{\omega_0}{2} t\right) \quad (43)$$

are the isolated system propagators. The reduced density evolution is now,

$$\begin{aligned} \mathbf{G}^<(t, t) &= \hbar^2 \mathbf{G}^{\text{OR}}(t, 0) \mathbf{G}^<(0, 0) \mathbf{G}^{\text{OA}}(0, t) e^{-t/(2\tau_{\text{SE}})} \\ &+ \int_0^t dt_i \mathbf{G}^{\text{OR}}(t, t_i) \mathbf{\Sigma}_{\text{sym.}}^<(t_i) \mathbf{G}^{\text{OA}}(t_i, t) e^{-(t-t_i)/(2\tau_{\text{SE}})}, \end{aligned} \quad (44)$$

which is similar to the GLBE [14, 15]. It is easy to see that the introduction of negative (positive) imaginary parts in the diagonal energies of the effective Hamiltonian produces decay (growth) rates of the elements of the density function which, being fictitious, must be compensated by a fictitious injection self-energy

$$\Sigma_{\text{fic.},ij}^<(t_i) = -\hbar \text{Im}(\Sigma_{\text{fic.},ii}^R + \Sigma_{\text{fic.},jj}^R) G_{ij}^<(t_i, t_i). \quad (45)$$

In our case, this results in an injection that includes the compensation effects for the symmetrized interaction

$$\begin{aligned}\Sigma_{\text{sym.}}^<(t_i) &= \Sigma^<(t_i) + \Sigma_{\text{fic.}}^<(t_i) \\ &= \begin{pmatrix} 0 & 0 \\ 0 & 2\Gamma_V \hbar \left(\frac{i}{\hbar} f_3\right) + 2\Gamma_U \hbar G_{22}^<(t_i, t_i) \end{pmatrix} \\ &+ \begin{pmatrix} \Gamma_{\text{SE}} \hbar G_{11}^<(t_i, t_i) & 0 \\ 0 & -\Gamma_{\text{SE}} \hbar G_{22}^<(t_i, t_i) \end{pmatrix}. \end{aligned} \quad (46)$$

Here, the second term is proportional to the system density functions $G_{ii}^<(t_i, t_i)$ injecting and extracting density on sites 1 and 2, respectively, to restore the real occupation. It is important to remark that the escape Γ_V given by V_{23} in Hamiltonian (3) or the process of current leads of Refs. [14, 25] are only compensated at a constant rate by the reservoirs. In this case, the injection self-energy is proportional to the density function in the environment. In contrast, for voltage probes, electron-phonon self-energies (as in Ref. [14]) or our Coulombic Γ_U require an immediate charge compensation. The same is true for the fictitious processes and this is indeed the situation of Eq. (46) where the injection self-energy is proportional to the instantaneous system density function. Thus, the fictitious injection self-energy compensates *instantaneously* the fictitious leak and injection of Eq. (40). This is more easily seen once Eq. (44) is integrated into a Trotter-type form, as we will discuss in connection to Eq. (76). The symmetrization method is, in essence, a redistribution of terms in the evolution equation (12) that has a simpler resolution.

We can rewrite the last expression to separate the processes that involve density relaxation (through injection and escape processes) and pure decoherence (through local energy fluctuations) as follows

$$\begin{aligned}\Sigma_{\text{sym.}}^<(t_i) &= \Sigma_i^<(t_i) + \Sigma_m^<(t_i) \\ &= i\Gamma_{\text{SE}} \left[2p_V \begin{pmatrix} 0 & 0 \\ 0 & (f_3 - \frac{\hbar}{i} G_{22}^<(t_i, t_i)) \end{pmatrix} \right. \\ &\quad \left. + \begin{pmatrix} \frac{\hbar}{i} G_{11}^<(t_i, t_i) & 0 \\ 0 & \frac{\hbar}{i} G_{22}^<(t_i, t_i) \end{pmatrix} \right]. \end{aligned} \quad (47)$$

Here

$$\frac{\hbar}{i} G_{22}^<(t_i, t_i) \equiv \frac{\hbar}{i} \int G_{22}^<(\varepsilon, t_i) \frac{d\varepsilon}{2\pi\hbar} = f_2(t_i) \quad (48)$$

and

$$\frac{\hbar}{i} G_{11}^<(t_i, t_i) = f_1(t_i), \quad (49)$$

while, remembering that according to Eqs. (24) and (30), $\Gamma_{\text{SE}} = \Gamma_U + \Gamma_V$, we define

$$p_V = \Gamma_V / \Gamma_{\text{SE}} \quad (50)$$

as the weight of the tunneling rate relative to the total SE interaction rate. Since the initial state has the site 2

occupied we have that

$$\frac{\hbar}{i} G_{ij}^<(0, 0) = \delta_{i2} \delta_{2j}. \quad (51)$$

Introducing Eq. (47) into Eq. (44) and using

$$\frac{1}{\tau_{\text{SE}}} \equiv \frac{2}{\hbar} \Gamma_{\text{SE}}, \quad (52)$$

we get two coupled equations for $G_{11}^<$ and $G_{22}^<$ as follows:

$$\begin{aligned}\frac{\hbar}{i} G_{11}^<(t, t) &= |\hbar G_{12}^{\text{OR}}(t, 0)|^2 e^{-t/(2\tau_{\text{SE}})} + \\ &\int |\hbar G_{12}^{\text{OR}}(t, t_i)|^2 e^{-(t-t_i)/(2\tau_{\text{SE}})} 2p_V \frac{dt_i}{2\tau_{\text{SE}}} [f_3 - \frac{\hbar}{i} G_{22}^<(t_i, t_i)] \\ &+ \int |\hbar G_{11}^{\text{OR}}(t, t_i)|^2 e^{-(t-t_i)/(2\tau_{\text{SE}})} \frac{dt_i}{2\tau_{\text{SE}}} [\frac{\hbar}{i} G_{11}^<(t_i, t_i)] \\ &+ \int |\hbar G_{12}^{\text{OR}}(t, t_i)|^2 e^{-(t-t_i)/(2\tau_{\text{SE}})} \frac{dt_i}{2\tau_{\text{SE}}} [\frac{\hbar}{i} G_{22}^<(t_i, t_i)], \end{aligned} \quad (53)$$

$$\begin{aligned}\frac{\hbar}{i} G_{22}^<(t, t) &= |\hbar G_{22}^{\text{OR}}(t, 0)|^2 e^{-t/(2\tau_{\text{SE}})} + \\ &\int |\hbar G_{22}^{\text{OR}}(t, t_i)|^2 e^{-(t-t_i)/(2\tau_{\text{SE}})} 2p_V \frac{dt_i}{2\tau_{\text{SE}}} [f_3 - \frac{\hbar}{i} G_{22}^<(t_i, t_i)] \\ &+ \int |\hbar G_{21}^{\text{OR}}(t, t_i)|^2 e^{-(t-t_i)/(2\tau_{\text{SE}})} \frac{dt_i}{2\tau_{\text{SE}}} [\frac{\hbar}{i} G_{11}^<(t_i, t_i)] \\ &+ \int |\hbar G_{22}^{\text{OR}}(t, t_i)|^2 e^{-(t-t_i)/(2\tau_{\text{SE}})} \frac{dt_i}{2\tau_{\text{SE}}} [\frac{\hbar}{i} G_{22}^<(t_i, t_i)]. \end{aligned} \quad (54)$$

In each equation, the first term is the probability that a particle initially at site 2 be found in site 1 (or 2) at time t having survived the interactions with the environment with a probability $e^{-t/(2\tau_{\text{SE}})}$. The second term describes the process of injection/escape of particles enabled by the hopping from/towards the reservoir, where the last of such processes occurred in the time range $(t_i, t_i + dt_i)$ with a probability $2p_V \frac{dt_i}{2\tau_{\text{SE}}}$. The injection (escape) at site 2 fills (empties) the site to level it up to the occupation factor f_3 . The third and fourth terms take into account the last process of measurement at time t_i due to the SE interaction with a probability $\frac{dt_i}{2\tau_{\text{SE}}}$. This confirms our interpretation that in Eq. (47) the dissipation processes are in $\Sigma_i^<(t)$ while $\Sigma_m^<(t)$ involves pure decoherence. It is clear that by iterating this formula, one gets a series in the form represented in Fig. 1(d).

In summary, Eqs. (53) and (54) are valid within the following assumptions: (a) The system is in the high temperature limit $V_{12}, U_{23}, V_{23}, V_B \ll k_B T$. (b) The environment is assumed to have a very fast dynamic as compared with that of the system $V_{12}, U_{23}, V_{23} \ll V_B$ (fast fluctuation regime). This is achieved through a specific model of the environment with a very wide band where this property shows up as a flat and broad local density of state at the “surface” site 3. These two are the central assumptions. The consequences of them are the

following limits: (c) The self-energy is described by the self-consistent second-order term. (d) The environment remains in equilibrium. (e) The retarded and advanced Green's functions are calculated from a non-Hermitian effective Hamiltonian which is independent of energy and constant in time.

The previous conditions allow us to develop a different strategy for the solution of the spatially inhomogeneous evolution equation (GLBE): We fictitiously symmetrize the effective Hamiltonian to impose an homogeneous decay of the coherent dynamics. Consequently, we compensate the resulting artificial injections and/or leaks based on a fictitious part in the injection self-energy.

D. Dynamics of a swapping gate

The solution of the coupled Eqs. (53) and (54) involves a Laplace transform. We consider a parameter range compatible with the spin problem where $f_3 \lesssim 1$ while we allow the tunneling relative weight p_V in the range $[0, 1]$. In a compact notation, the density function results as follows

$$\frac{\hbar}{i} G_{11}^<(t, t) = 1 - a_0 e^{-R_0 t} - a_1 \cos[(\omega + i\eta)t + \varphi_0] e^{-R_1 t}. \quad (55)$$

Here, the decay rates R_0 , R_1 , and η , and the oscillation frequency ω are real numbers associated with poles of the Laplace transform. The amplitude a_0 is also real while, when $\omega = 0$, the amplitude a_1 and the initial phase φ_0 acquire an imaginary component that warrants a real density. These observables have expressions in terms of adimensional functions of the fundamental parameters in the model. Denoting

$$x = \omega_0 \tau_{SE}, \quad (56)$$

and remembering that

$$p_V = \Gamma_V / \Gamma_{SE}, \quad (57)$$

we define

$$\chi(p_V, x) = \frac{1}{3} \left(x^2 - p_V^2 - \frac{1}{3} (1 - p_V)^2 \right), \quad (58)$$

and

$$\begin{aligned} \chi(p_V, x) = & \left\{ 4(1 - p_V) \left(9x^2 - 2(1 - p_V)^2 + 18p_V^2 \right) \right. \\ & + 12 \left[3 \left(4x^6 - \left((1 - p_V)^2 + 12p_V^2 \right) x^4 \right. \right. \\ & \left. \left. + 4p_V^2 \left(5(1 - p_V)^2 + 3p_V^2 \right) x^2 \right. \right. \\ & \left. \left. \left. - 4p_V^2 \left((1 - p_V)^2 - p_V^2 \right)^2 \right) \right]^{\frac{1}{2}} \right\}^{\frac{1}{3}}. \quad (59) \end{aligned}$$

The observable “frequency”,

$$\omega + i\eta = \frac{\sqrt{3}}{2x} \left(\frac{1}{6} \chi(p_V, x) + 6 \frac{\phi(p_V, x)}{\chi(p_V, x)} \right) \omega_0, \quad (60)$$

is purely real or imaginary, i.e. $\omega\eta \equiv 0$. Also,

$$R_0 = \left(6 \frac{\phi(p_V, x)}{\chi(p_V, x)} - \frac{1}{6} \chi(p_V, x) + p_V + \frac{1}{3} (1 - p_V) \right) \frac{1}{\tau_{SE}}, \quad (61)$$

$$R_1 = \frac{3}{2} \left(p_V + \frac{1}{3} (1 - p_V) \right) \frac{1}{\tau_{SE}} - \frac{R_0}{2}, \quad (62)$$

and

$$a_0 = \frac{1}{2} \frac{2(\omega^2 - \eta^2) + 2R_1^2 - \omega_0^2}{(\omega^2 - \eta^2) + (R_0 - R_1)^2}, \quad (63)$$

$$a_2 = \frac{1}{2(\omega + i\eta)} \times \frac{(2R_0 R_1 - \omega_0^2)(R_0 - R_1) + 2(\omega^2 - \eta^2) R_0}{(\omega^2 - \eta^2) + (R_0 - R_1)^2}, \quad (64)$$

$$a_3 = \frac{1}{2} \frac{\omega_0^2 + 2R_0^2 - 4R_0 R_1}{(\omega^2 - \eta^2) + (R_0 - R_1)^2}, \quad (65)$$

$$a_1^2 = a_2^2 + a_3^2, \quad \tan(\phi_0) = -\frac{a_2}{a_3}. \quad (66)$$

The oscillation frequency ω in Eq. (60) has a critical point x_c at a finite value of x showing a quantum dynamical phase transition for which ω and η in Eq. (55) exchange their roles as being zero and having a finite value, respectively. A full discussion of this issue for a spin system is presented in Ref. [17]. Here, the dynamical behavior changes from a swapping phase to an overdamped phase. This last regime can be associated with the quantum Zeno effect [28] where frequent projective measurements prevent the quantum evolution. Here, this is a dynamical effect [29, 30] produced by interactions with the environment that freeze the system oscillation.

Figure 2 shows typical curves of $\frac{\hbar}{i} G_{11}^<(t, t)$ in the swapping phase. The different colors correspond to different SE interactions, $p_V = 0, 0.5$, and 1, which are Coulomb ($\Gamma_V = 0$), isotropic ($\Gamma_V = \Gamma_U$), and pure tunneling ($\Gamma_U = 0$) interaction rates. The hopping interaction does not conserve the net energy in the system inducing a dissipation which is manifested through the nonconservation of the number of particles in the system. This is the case of $p_V \neq 0$ where the final state of the system has the occupation probability of the sites equilibrated with the bath occupation (f_3). In Fig. 2, this is manifested as the asymptotic normalized density (occupation probability) of 1. However, if $p_V = 0$, tunneling is forbidden and the system goes to an internal quasiequilibrium, i.e., the local excitation is spread inside the system. In this case the asymptotic occupation probability of site 1 is 1/2.

IV. STROBOSCOPIC REPRESENTATION OF THE INTERACTION PROCESSES

Equation. (37) has two main difficulties for a numerical implementation: The first is the evaluation of the system

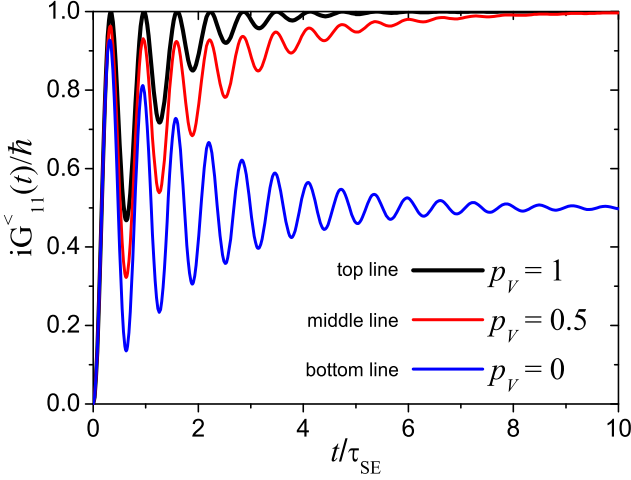


FIG. 2: (Color online) Occupation probability $iG_{11}^<(t)/\hbar$ to find at site 1 a particle initially at site 2. Each line corresponds to different kinds, p_V , of SE interactions. The plots correspond to $x = V_{12}\tau_{\text{SE}}/\hbar = 10$ belonging to the swapping phase and $f_3 = 1$.

nonunitary propagators under inhomogeneous perturbations; the second is to keep track of all the previous states of the system to enable the integration over past times. We will show that the decay homogenization enables the implementation of an efficient numerical algorithm. First of all, we identify in expression (44) that $e^{-t/(2\tau_{\text{SE}})} = s(t)$ is the system's survival probability to the environment interruption, i.e., the probability that the system remains coherent, and $dt_i/(2\tau_{\text{SE}}) = q(t_i)dt_i$ is the “interruption” probability in a differential time around t_i . The interaction of the environment is discretized in intervals τ_{str} where it acts instantaneously. This stroboscopic interaction leads to

$$s(t) = (1-p)^{n(t)}, \quad (67)$$

$$q(t) = \sum_{m=1}^{\infty} p \delta(t - m\tau_{\text{str}}), \quad (68)$$

where

$$n(t) = \text{int}(t/\tau_{\text{str}}). \quad (69)$$

Here, the stroboscopic interruptions may occur at the discrete times $m\tau_{\text{str}}$ with a probability p . At time t there were $n(t)$ possible interruptions. In the joint limit $\tau_{\text{str}} \rightarrow 0$ and $p \rightarrow 0$ such that

$$p/\tau_{\text{str}} = 1/(2\tau_{\text{SE}}), \quad (70)$$

we recover the continuous expression (see the Appendix).

Introducing Eqs. (67) and (68) into the reduced den-

sity expression (44) we obtain

$$\begin{aligned} \mathbf{G}^<(t, t) &= \hbar^2 \mathbf{G}^{\text{OR}}(t, 0) \mathbf{G}^<(0, 0) \mathbf{G}^{\text{OA}}(0, t) (1-p)^{n(t)} \\ &\quad + \int_0^t dt_i \tau_{\text{SE}} \sum_{m=1}^{\infty} \delta(t_i - t_m) \\ &\quad \times \mathbf{G}^{\text{OR}}(t, t_i) \Sigma_{\text{sym.}}^<(t_i) \mathbf{G}^{\text{OA}}(t_i, t) p (1-p)^{n(t-t_i)}, \end{aligned} \quad (71)$$

and rewriting we have

$$\begin{aligned} \mathbf{G}^<(t, t) &= \hbar^2 \mathbf{G}^{\text{OR}}(t, 0) \mathbf{G}^<(0, 0) \mathbf{G}^{\text{OA}}(0, t) (1-p)^n \\ &\quad + \hbar^2 \sum_{m=1}^n \mathbf{G}^{\text{OR}}(t, t_m) \delta \mathbf{G}_{\text{inj.}}^<(t_m, t_m) \mathbf{G}^{\text{OA}}(t, t_m) \\ &\quad \times p (1-p)^{n-m}, \end{aligned} \quad (72)$$

where $n = n(t)$, $t_m = m\tau_{\text{str.}}$, and

$$\delta \mathbf{G}_{\text{inj.}}^<(t, t) = \frac{2\tau_{\text{SE}}}{\hbar^2} \Sigma_{\text{sym.}}^<(t). \quad (73)$$

In this picture, the evolution between interruptions is governed by the system's propagators

$$\mathbf{G}^{\text{OR}}(t, 0) = -\frac{i}{\hbar} \exp[-i\mathbf{H}_S t/\hbar] \quad (74)$$

and

$$\mathbf{G}^{\text{OA}}(0, t) = \mathbf{G}^{\text{OR}}(t, 0)^\dagger. \quad (75)$$

The spin bath stroboscopically interrupts the system evolution producing the decay of the coherent beam. This decay is compensated through the reinjection of probability (or eventually of coherences) expressed in the *instantaneous interruption function* $\delta \mathbf{G}_{\text{inj.}}^<(t, t)$ which also contains actual injection (decay) from (to) the bath.

The first term in the rhs of Eq. (72) is the coherent system evolution weighted by its survival probability $(1-p)^n$. This is the upper branch in Fig. 3. The second term is the incoherent evolution involving all the decoherent branches. The m -th term in the sum represents the evolution that had its *last* interruption at $m\tau_{\text{str.}}$ and since then survived coherently until $n\tau_{\text{str.}}$. Each of these terms is represented in Fig. 3 by all the branches with an interrupted state (gray dot, red online) at the hierarchy level m after which they survive without further interruptions until $n\tau_{\text{str.}}$. This representation has an immediate resemblance to that introduced by Pascazio and Namiki to justify the dynamical Zeno effect [30].

As mentioned above, the solutions of Eqs. (72) and (44) are both computationally demanding since they involve the storage of all the previous steps and reiterated summations. Thus, taking advantage of the self-similarity of the hierarchy levels in the interaction with the environment, we rearrange expression (72) into a form optimized for numerical computation,

$$\begin{aligned} \frac{1}{\hbar^2} \mathbf{G}^<(t_{n+1}, t_{n+1}) &= \\ &\mathbf{G}^{\text{OR}}(t_{n+1}, t_n) \mathbf{G}^<(t_n, t_n) \mathbf{G}^{\text{OA}}(t_n, t_{n+1}) (1-p) \\ &+ \mathbf{G}^{\text{OR}}(t_{n+1}, t_n) \delta \mathbf{G}_{\text{inj.}}^<(t_n, t_n) \mathbf{G}^{\text{OA}}(t_n, t_{n+1}) p. \end{aligned} \quad (76)$$

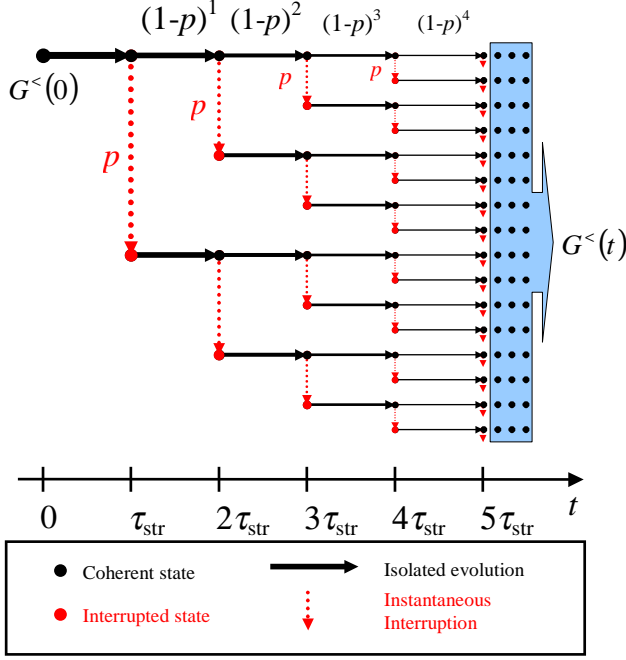


FIG. 3: (Color online) Quantum branching sequence for the stroboscopic evolution. Gray (red) dots represent states with interrupted (incoherent) evolution while the black dots are coherent with their predecessor. The horizontal continuous arrows represent the isolated evolution and the vertical dashed lines are the instantaneous interruptions. Notice the self-similar structure.

This equation provides a new computational procedure that only requires the storage of the density function at a single previous step. Besides, it avoids random averages required in models that include decoherence through stochastic or kicked-like perturbations [31, 32]. This strategy is being implemented in our group in various cases involving quantum dynamics of many spin systems in the presence of dissipation processes and decoherence. Equation (76) manifests that the fictitious self-energy, proportional to $G_{ii}^<(t_n, t_n)$, compensates instantaneously the fictitious leaks and injection of Eq. (40). The conceptual consistency of the approach is illustrated by choosing $\delta \mathbf{G}_{\text{inj}}^<(t_n, t_n) \equiv \mathbf{G}^<(t_n, t_n)$: one recovers a coherent isolated evolution.

V. APPLICATION TO SPIN SYSTEMS

We apply this procedure to the spin system of Ref. [17] providing a first principle derivation of the phenomenological equations employed there. We consider a system with $M = 2$ spins $1/2$ coupled to a spin environment with the following Hamiltonian $\hat{\mathcal{H}} = \hat{\mathcal{H}}_S + \hat{\mathcal{H}}_E + \hat{\mathcal{H}}_{SE}$, where

the system Hamiltonian $\hat{\mathcal{H}}_S$ is

$$\begin{aligned} \hat{\mathcal{H}}_S &= \hbar\omega_L (\hat{I}_1^z + \hat{I}_2^z) + \frac{1}{2}b_{12} (\hat{I}_1^+ \hat{I}_2^- + \hat{I}_1^- \hat{I}_2^+) \\ &= \hbar\omega_L (\hat{I}_1^z + \hat{I}_2^z) + b_{12} (\hat{I}_1^x \hat{I}_2^x + \hat{I}_1^y \hat{I}_2^y). \end{aligned} \quad (77)$$

Here, the first term is the Zeeman energy and the second term gives a flip-flop or XY spin-spin interaction. The environment Hamiltonian is described by

$$\hat{\mathcal{H}}_E = \sum_{i \geq 3} \hbar\omega_L \hat{I}_i^z + \sum_{\substack{i \geq 3 \\ j > i}} \frac{1}{2}b_{ij} (\hat{I}_i^+ \hat{I}_j^- + \hat{I}_i^- \hat{I}_j^+), \quad (78)$$

and for the SE interaction we have

$$\hat{\mathcal{H}}_{SE} = a_{23} \hat{I}_2^z \hat{I}_3^z + \frac{1}{2}b_{23} (\hat{I}_2^+ \hat{I}_3^- + \hat{I}_2^- \hat{I}_3^+), \quad (79)$$

where this spin-spin interaction is Ising if $b_{23}/a_{23} = 0$, and XY , isotropic (Heisenberg), or the truncated dipolar (secular) if $a_{23}/b_{23} = 0, 1, -2$, respectively.

We map the spin system into a fermionic system using the Jordan-Wigner transformation (JWT) [33],

$$\hat{I}_i^+ = \hat{c}_i^+ \exp \left\{ i\pi \sum_{j=1}^{i-1} \hat{c}_j^+ \hat{c}_j \right\}. \quad (80)$$

The previous Hamiltonians become

$$\hat{\mathcal{H}}_S = \hbar\omega_L (\hat{c}_1^+ \hat{c}_1 + \hat{c}_2^+ \hat{c}_2 - 1) + \frac{1}{2}b_{12} (\hat{c}_1^+ \hat{c}_2 + \hat{c}_2^+ \hat{c}_1), \quad (81)$$

$$\hat{\mathcal{H}}_E = \sum_{i \geq 3} \hbar\omega_L (\hat{c}_i^+ \hat{c}_i - \frac{1}{2}1) + \sum_{\substack{i \geq 3 \\ j > i}} \frac{1}{2}b_{ij} (\hat{c}_i^+ \hat{c}_j + \hat{c}_j^+ \hat{c}_i), \quad (82)$$

$$\hat{\mathcal{H}}_{SE} = a_{23} (\hat{c}_2^+ \hat{c}_2 - \frac{1}{2}) (\hat{c}_3^+ \hat{c}_3 - \frac{1}{2}) + \frac{1}{2}b_{23} (\hat{c}_2^+ \hat{c}_3 + \hat{c}_3^+ \hat{c}_2). \quad (83)$$

Here, the system interacts with the environment through site 3 (the surface site of the bath). In the last Hamiltonians, the terms proportional to the identity do not contribute to the dynamics because they only change the total energy by a constant number. This Hamiltonian describes a standard cross polarization experiment (swapping gate) in NMR [17, 19]. In this experiment, site 1 is a ^{13}C and site 2 is a ^1H while the environment is a ^1H spin bath. The typical experimental Hartmann-Hahn condition [17, 19] equals the values of the effective energies at the ^{13}C and the ^1H sites to optimize the polarization transfer. The SE interaction has terms linear in the number operators $\hat{c}_2^+ \hat{c}_2$ and $\hat{c}_3^+ \hat{c}_3$, that only change the energy of sites 2 and 3, respectively. Thus, the Hartmann-Hahn implementation, compensates the change of energy produced by the environment through these linear terms. Finally, we have Hamiltonians equivalent to those in Eqs. (1-3) where the site energies are

equal, and $V_{12} = -\frac{b_{12}}{2}$, $V_{ij} = -\frac{b_{ij}}{2}$, $U_{23}^{(\text{dir.})} = a_{23}$, and $U_{23}^{(\text{exch.})} = 0$.

The spin dynamics of the system is described by the spin correlation function [20, 27] as follows:

$$P_{i2}(t) = \frac{\langle \Psi_{\text{eq.}} | \hat{I}_i^z(t) \hat{I}_2^z(0) | \Psi_{\text{eq.}} \rangle}{\langle \Psi_{\text{eq.}} | \hat{I}_2^z(0) \hat{I}_2^z(0) | \Psi_{\text{eq.}} \rangle}, \quad (84)$$

which gives the local polarization at time t on the i -th spin with an initial local excitation on the 2-nd spin at time $t = 0$. Here, $|\Psi_{\text{eq.}}\rangle$ is the thermodynamical many-body equilibrium state and

$$\hat{I}_i^z(t) = e^{i\hat{H}t/\hbar} \hat{I}_i^z e^{-i\hat{H}t/\hbar} \quad (85)$$

are the spin operators in the Heisenberg representation. After the JWT, the initial local excitation on site 2 is described by the nonequilibrium state

$$|\Psi_{\text{n.e.}}\rangle = \hat{c}_2^+ |\Psi_{\text{eq.}}\rangle. \quad (86)$$

In the experimental high temperature regime, $k_B T$ much larger than any energy scale of the system, the spin correlation function becomes

$$P_{i2}(t) = \frac{2\hbar}{1} G_{ii}^<(t, t) - 1. \quad (87)$$

Notice that $G_{ii}^<(t, t)$ implicitly depends on the initial local excitation at site 2. Here, $G_{ii}^<(t, t)$ is the reduced density function of sites 1 and 2 and can be split into the contributions $G_{ii}^{<(N)}(t_2, t_1)$ from each subspace with N particles (or equivalently N spins up) in the following way [27]:

$$G_{ii}^<(t, t) = \sum_{N=1}^M \frac{\binom{M-1}{N-1}}{2^{M-1}} G_{ii}^{<(N)}(t, t), \quad (88)$$

and analogous for the hole density function. The initial condition in this picture is described by

$$G_{ij}^{<(N)}(0, 0) = \frac{i}{\hbar} \left(\frac{N-1}{M-1} \delta_{ij} + \frac{M-N}{M-1} \delta_{i2} \delta_{2j} \right), \quad (89)$$

where the first term is the equilibrium density (identical occupation for all the sites) and the second term is the nonequilibrium contribution where only site 2 is excited. Thus, we have an expression such as (12) for each N -th subspace (see Ref. [27]). For this two-spin system, as we showed in [27], the -1 term of Eq. (87) is canceled out by the background evolution, i.e., the evolution of the first term of Eq. (89) plus the evolution of the second term of Eq. (12) for the $N = 2$ subspace. As a consequence, the observable dynamics only depends on the initial local excitation at site 2,

$$G_{ij}^{<(1)}(0, 0) = \frac{i}{\hbar} \delta_{i2} \delta_{2j}, \quad (90)$$

and evolves in the first particle subspace,

$$P_{i2}(t) = \frac{\hbar}{1} G_{ii}^{<(1)}(t, t). \quad (91)$$

Finally, the solution of the polarization $P_{12}(t)$ is the same as that obtained in Eq. (55).

By substituting in the present microscopic model $\Gamma_{XY} \leftrightarrow \Gamma_V$ and $\Gamma_{ZZ} \leftrightarrow \Gamma_U$, we obtain the same dynamics as that found in Ref. [17] for a phenomenological spin model. There, we showed that such a solution presents a quantum dynamical phase transition in fair agreement with the phenomenon observed experimentally [18].

VI. CONCLUSIONS

We have shown a method that involves the transformation of the density function expressed in the Danielewicz integral form into a generalized Landauer-Büttiker equation. This was possible by resorting to Wigner energy-time variables to perform the fast fluctuation approximation for the environment which leads to interactions local in time. Further on, we effectively symmetrized the system-environment interactions transforming them into a spatially homogeneous process. This has a uniform system-environment interaction rate leading to a simple non-Hermitian propagator. The original multiexponential decay processes are recovered by an injection density function. Moreover, through discretization of the GLBE, we built a stroboscopic process which is the basis for an optimal numerical algorithm where the quantum dynamics is calculated in discrete time steps. Finally, we applied these techniques to a spin system giving a microscopic derivation that justifies the stroboscopic model used in Ref. [17] to explain the experimentally observed quantum dynamical phase transition.

APPENDIX A: RECOVERING THE CONTINUOUS PROCESS

In order to recover the continuous expression (44) from the stroboscopic one (72) we notice that if $n(t) = n$, we can write Eq. (67) as

$$s(t) = (1-p)^{\frac{(n\tau_{\text{str.}})}{\tau_{\text{str.}}}} = \left(1 - \frac{\tau_{\text{str.}}}{2\tau_{\text{SE}}}\right)^{(n\tau_{\text{str.}})/\tau_{\text{str.}}}. \quad (A1)$$

If $t = n\tau_{\text{str.}}$ then

$$s(t) = \left(1 - \frac{\tau_{\text{str.}}}{2\tau_{\text{SE}}}\right)^{t/\tau_{\text{str.}}}. \quad (A2)$$

By taking the limit $\tau_{\text{str.}} \rightarrow 0$ the variable t becomes continuous yielding

$$\begin{aligned} s(t) &= \lim_{\tau_{\text{str.}} \rightarrow 0} \left(1 - \frac{\tau_{\text{str.}}}{2\tau_{\text{SE}}}\right)^{t/\tau_{\text{str.}}} \\ &= \exp[-t/(2\tau_{\text{SE}})], \end{aligned} \quad (A3)$$

recovering the continuous expression for $s(t)$.

By substituting $p = \tau_{\text{str.}}/(2\tau_{\text{SE}})$ in Eq. (68) we have

$$q(t) = \frac{1}{2\tau_{\text{SE}}} \sum_{m=1}^{\infty} \tau_{\text{str.}} \delta(t - m\tau_{\text{str.}}). \quad (\text{A4})$$

In the limit $\tau_{\text{str.}} \rightarrow 0$, $t_m = m\tau_{\text{str.}}$ becomes a continuous variable and we can convert the sum into an integral, leading to

$$q(t) = \frac{1}{2\tau_{\text{SE}}} \int_0^{\infty} \tau_{\text{str.}} \delta(t - t_m) \frac{dt_m}{\tau_{\text{str.}}} = \frac{1}{2\tau_{\text{SE}}}. \quad (\text{A5})$$

The continuous expression of the GLBE (44) is then obtained.

-
- [1] C. H. Bennett and D. P. Di Vincenzo, *Nature* **404**, 247 (2000).
 - [2] J. R. Petta, A. C. Johnson, J. M. Taylor, E. A. Laird, A. Yacoby, M. D. Lukin, C. M. Marcus, M. P. Hanson, and A. C. Gossard, *Science* **309**, 2180 (2005).
 - [3] M. Poggio, G. M. Steeves, R. C. Myers, Y. Kato, A. C. Gossard, and D. D. Awschalom, *Phys. Rev. Lett.* **91**, 207602 (2003).
 - [4] J. M. Taylor, A. Imamoglu, and M. D. Lukin, *Phys. Rev. Lett.* **91**, 246802 (2003).
 - [5] H. M. Pastawski, P. R. Levstein, G. Usaj, J. Raya, and J. A. Hirschinger, *Physica A* **283**, 166 (2000).
 - [6] C. J. Myatt, B. E. King, Q. A. Turchette, C. A. Sackett, D. Kielpinski, W. M. Itano, C. Monroe, and D. J. Wineland, *Nature* **403**, 269 (2000).
 - [7] S. A. Gurvitz, L. Fedichkin, D. Mozyrsky, and G. P. Berman, *Phys. Rev. Lett.* **91**, 066801 (2003).
 - [8] W. H. Zurek, *Rev. Mod. Phys.* **75**, 715 (2003).
 - [9] J. M. Taylor, H.-A. Engel, W. Dür, A. Yacoby, C. M. Marcus, P. Zoller, and M. D. Lukin, *Nature Phys.* **1**, 177 (2005).
 - [10] J. J. L. Morton, A. M. Tyryshkin, A. Ardavan, S. C. Benjamin, K. Porfyrakis, S. A. Lyon, and G. A. D. Briggs, *Nature Phys.* **2**, 40 (2006).
 - [11] A. Abragam, *The Principles of Nuclear Magnetism* (Clarendon Press, Oxford, 1961); R. R. Ernst, G. Bodenhausen, and A. Wokaun, *Principles of Nuclear Magnetic Resonance in One and Two Dimensions* (Oxford University Press, Oxford, 1987).
 - [12] L. V. Keldysh, *Zh. Eksp. Teor. Fiz.* **47**, 1515 (1964) [*Sov. Phys. JETP* **20**, 1018 (1965)].
 - [13] P. Danielewicz, *Ann. Phys.* **152**, 239 (1984).
 - [14] H. M. Pastawski, *Phys. Rev. B* **46**, 4053 (1992) [see Eq. (4.11)].
 - [15] H. M. Pastawski, *Phys. Rev. B* **44**, 6329 (1991) [see Eq. (3.7)].
 - [16] S. Vorojtsov, E. R. Mucciolo, and H. U. Baranger, *Phys. Rev. B* **71**, 205322 (2005).
 - [17] G. A. Álvarez, E. P. Danieli, P. R. Levstein, and H. M. Pastawski, *J. Chem. Phys.* **124**, 194507 (2006).
 - [18] P. R. Levstein, G. Usaj, and H. M. Pastawski, *J. Chem. Phys.* **108**, 2718 (1998).
 - [19] L. Müller, A. Kumar, T. Baumann, and R. R. Ernst, *Phys. Rev. Lett.* **32**, 1402 (1974).
 - [20] E. P. Danieli, H. M. Pastawski, and P. R. Levstein, *Chem. Phys. Lett.* **384**, 306 (2004).
 - [21] The characters in bold font are matrix representations of the respective operator.
 - [22] P. R. Levstein, H. M. Pastawski, and J. L. D'Amato, *J. Phys.: Condens. Matter* **2** 1781 (1990).
 - [23] J. L. D'Amato and H. M. Pastawski, *Phys. Rev. B* **41**, 7411 (1990).
 - [24] E. Rufeil Fiori and H. M. Pastawski, *Chem. Phys. Lett.* **420** 35 (2006).
 - [25] G. Stefanucci and C.-O. Almbladh, *Phys. Rev. B* **69**, 195318 (2004).
 - [26] E. P. Danieli, G. A. Álvarez, P. R. Levstein, and H. M. Pastawski, *Solid State Commun.* **141**, 422 (2007).
 - [27] E. P. Danieli, H. M. Pastawski, and G. A. Álvarez, *Chem. Phys. Lett.* **402**, 88 (2005).
 - [28] B. Misra and E. C. G. Sudarshan, *J. Math. Phys.* **18**, 756 (1977).
 - [29] H. M. Pastawski and G. Usaj, *Phys. Rev. B* **57**, 5017 (1998).
 - [30] S. Pascazio and M. Namiki, *Phys. Rev. A* **50**, 4582 (1994).
 - [31] G. Teklemariam, E. M. Fortunato, C. C. López, J. Emerson, J. P. Paz, T. F. Havel, and D. G. Cory, *Phys. Rev. A* **67**, 062316 (2003).
 - [32] J. Dalibard, Y. Castin, and K. Mølmer, *Phys. Rev. Lett.* **68**, 580 (1992).
 - [33] E. H. Lieb, T. Schultz, and D. C. Mattis, *Ann. Phys.* **16**, 407 (1961).